OPTIMAL SENSOR DEPLOYMENT FOR 3D AOA TARGET LOCALIZATION

Sheng Xu[⋆] *and Kutluyıl Doğançay*[⋆◊]

[⋆]Institute for Telecommunications Research, [◊]School of Engineering
University of South Australia, Australia

ABSTRACT

This paper investigates the problem of how to improve angle-of-arrival (AOA) target localization accuracy by finding an optimal AOA sensor deployment strategy in 3D space. Under the assumption of constant absolute elevation angles for the sensors, a novel and simple optimal sensor deployment criterion is proposed based on minimizing the trace of inverse Fisher information matrix. Our analysis shows that when sensor elevation angles equal $\pm 42.2869^o$ and twice of azimuth angles have equal angular distribution with uniform distance from the target and equal noise covariance, the lowest mean squared error is achieved. Besides, with more sensors placed closer to the target, a lower mean squared error is attained. Simulation examples are presented to verify the effectiveness of the developed optimality criterion.

Index Terms— Angle-of-arrival localization, Fisher information matrix, Cramér-Rao lower bound, optimal sensor deployment.

1. INTRODUCTION

Angle-of-arrival (AOA) localization is a classical passive target localization method which has been widely used in both military and civilian applications. A weighted least-squared estimator was first used for AOA localization in 2D that can be considered as an approximate maximum likelihood estimator (MLE) in the presence of small independent noise [1]. The pseudo-linear estimator (PLE), a linear least squared estimator with a closed-form solution, was designed in [2] for target localization via bearing observations. In [3], an improved PLE with bias compensation strategy was developed for bearings-only passive target localization. The extended Kalman filter is another useful method for the nonlinear AOA target localization problem [4]. The application of the range-parameterised EKF with improved stability was considered in [5]. In [6] an instrumental variable estimator was presented for 3D AOA target localization. Central to AOA localization is triangulation of the angle measurements acquired by many sensors, which means that sensor measurements and placements play a crucial role for target localization [7].

Optimal sensor placement strategies have been studied extensively. In [8], the Cramér-Rao lower bound (CRLB) is used to evaluate the estimation performance for the bearing-only localization method. In [9] the problem of how to get an accurate estimation result was transformed into how to maximize the determinant of Fisher information matrix (FIM). Thus, a relationship between estimation performance and the FIM was established. An optimal angular sensor deployment criterion based on D-optimum method (maximizing the determinant of the FIM) [10] for AOA target localization was proposed and proven [11].

However, the results in these previous works can only be used for 2D localization. In 3D, as the FIM becomes more complex, the development of optimal sensor deployment for AOA localization becomes more challenging and has not been fully addressed. In [12], a unified optimal sensor placement strategy for bearing-only, range-only, or received-signal-strength sensors in 2D and 3D was proposed based on framework theory to maximize the determinant of the FIM. In [13] an A-optimum method (minimizing the trace of CRLB) was applied to optimal sensor placement for 3D underwater target localization. In [14], a simple and clear result was obtained by minimizing the trace of the CRLB for elliptic time-of-arrival optimal receiver placement in both 2D and 3D. The optimal sensor geometry was described by a numerical solution.

In this paper, we focus on the optimal sensor deployment for 3D AOA target localization when all sensors have the same absolute elevation angle from the target. The FIM is developed by analyzing the 3D sensor measurement model. A new and simple optimal angular sensor deployment criterion is proposed based on an inequality property of the A-optimality criterion [10]. This result can be easily used for any 3D AOA target localization algorithm that is approximately efficient. The paper is organized as follows. Section 2 describes the 3D AOA sensor deployment optimization problem. The main results of this paper are presented in Section 3. Section 4 introduces an estimation algorithm based on the extended Kalman filter (EKF) and presents simulation examples for verifying the results presented in Section 3. Section 5 draws the conclusion.

2. PROBLEM FORMULATION

Fig. 1 shows the kth AOA sensor measurements for target localization in 3D comprised of an azimuth angle θ_k and an elevation angle ϕ_k.

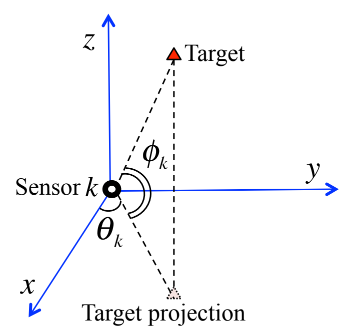

Fig. 1: AOA sensor measurements in 3D space.

The ideal (noiseless) angle measurements can be written as:

$$\theta_k = \arctan \frac{y_e - y_k}{x_e - x_k}, \quad -\pi < \theta_k \le \pi \tag{1}$$

$$\phi_k = \arctan \frac{z_e - z_k}{||[x_e, y_e] - [x_k, y_k]||}, \quad -\frac{\pi}{2} < \phi_k \le \frac{\pi}{2} \tag{2}$$

where the real target location is $[x_e, y_e, z_e]$ and the kth sensor is located at $[x_k, y_k, z_k]$ in 3D Cartesian coordinates. The distance between the target and the kth sensor is d_k and the projected distance in the xy plane is $d_{xyk} = ||[x_e, y_e] - [x_k, y_k]|| = d_k \cos\phi_k$ where $||\cdot||$ means the Euclidean norm.

The main objective is to locate the target in 3D from multiple angle measurements collected by sensors. The sensor deployment can influence the localization performance significantly [12]. Thus we first need to determine how the sensor deployment affects the target localization accuracy.

The noisy angle measurements of sensor k can be written as

$$\boldsymbol{z}_k = [\theta_k, \phi_k]^T + \boldsymbol{n}_k \tag{3}$$

where $\boldsymbol{z}_k$ is the sensor measurement at sensor k and $\boldsymbol{n}_k$ is the additive zero-mean independent Gaussian noise vector. The noise variances for θ_k and ϕ_k measurements are σ_θ^2 and σ_ϕ^2, respectively. If there are N sensors in the target localization system, the sensor measurement covariance is

$$\boldsymbol{\Sigma} = \begin{bmatrix} \sigma_\theta^2 \boldsymbol{I}_{N\times N} & 0 \\ 0 & \sigma_\phi^2 \boldsymbol{I}_{N\times N} \end{bmatrix}_{2N\times 2N}. \tag{4}$$

In this paper, we assume i.i.d. noise, i.e., $\sigma_\theta^2 = \sigma_\phi^2 = \sigma^2$. Then we can write the Jacobian of measurement errors evaluated at the true azimuth and elevation angles as [6]

$$\boldsymbol{J}_k = \begin{bmatrix} \frac{\sin\theta_1}{d_{xy1}} & \frac{-\cos\theta_1}{d_{xy1}} & 0 \\ \vdots & \vdots & \vdots \\ \frac{\sin\theta_N}{d_{xyN}} & \frac{-\cos\theta_N}{d_{xyN}} & 0 \\ \frac{\sin\phi_1\cos\theta_1}{d_1} & \frac{\sin\phi_1\sin\theta_1}{d_1} & \frac{-\cos^2\phi_1}{d_{xy1}} \\ \vdots & \vdots & \vdots \\ \frac{\sin\phi_N\cos\theta_N}{d_N} & \frac{\sin\phi_N\sin\theta_N}{d_N} & \frac{-\cos^2\phi_N}{d_{xyN}} \end{bmatrix}_{2N\times 3}. \tag{5}$$

The Fisher information matrix $\boldsymbol{\Phi}$ is given by [15]:

$$\boldsymbol{\Phi} = \boldsymbol{J}_k^T \boldsymbol{\Sigma}^{-1} \boldsymbol{J}_k \tag{6a}$$

$$= \frac{1}{\sigma^2} \boldsymbol{J}_k^T \boldsymbol{J}_k. \tag{6b}$$

The FIM is shown in (7) at the bottom of this page. In the next section we study how to deploy the sensors in order to optimize the FIM for estimation error minimization.

3. OPTIMAL SENSOR DEPLOYMENT

In order to get an accurate target location, we need to define a measure of estimation error. There are different criteria for this purpose. In this work we adopt the A-optimum criterion [10] which is equivalent to minimizing the trace of the CRLB. We assume a uniform target range from the sensors, i.e., $d_1 = d_2 = \cdots = d_N$. Then the optimal sensor deployment problem reduces to finding the optimal ϕ_k and θ_k that minimize the trace of the CRLB.

Note that

$$CRLB = \boldsymbol{\Phi}^{-1}. \tag{8}$$

Based on the Courant-Fischer-Weyl min-max principle [16] and the result in [13] [14], the trace of the CRLB cannot be smaller than the sum of the FIM's reciprocal diagonal elements. Thus we have

$$\begin{aligned} \text{tr}(CRLB) \geqslant \sigma^2 \Bigg(& \frac{1}{\sum_{k=1}^{N}\left(\frac{\sin^2\theta_k}{d_k^2\cos^2\phi_k} + \frac{\sin^2\phi_k\cos^2\theta_k}{d_k^2}\right)} \\ & + \frac{1}{\sum_{k=1}^{N}\left(\frac{\cos^2\theta_k}{d_k^2\cos^2\phi_k} + \frac{\sin^2\phi_k\sin^2\theta_k}{d_k^2}\right)} + \frac{1}{\sum_{k=1}^{N}\frac{\cos^2\phi_k}{d_k^2}} \Bigg) \end{aligned} \tag{9}$$

where tr$(CRLB)$ means the trace of the CRLB. The inequality in (9) becomes an equality only when $\boldsymbol{\Phi}$ is a diagonal matrix, which implies

$$\sum_{k=1}^{N}\left(\frac{-\sin\theta_k\cos\theta_k}{d_k^2\cos^2\phi_k} + \frac{\sin^2\phi_k\sin\theta_k\cos\theta_k}{d_k^2}\right) = 0 \tag{10a}$$

$$\sum_{k=1}^{N}\frac{-\sin\phi_k\cos\theta_k\cos\phi_k}{d_k^2} = 0 \tag{10b}$$

$$\sum_{k=1}^{N}\frac{-\sin\phi_k\sin\theta_k\cos\phi_k}{d_k^2} = 0. \tag{10c}$$

In order to simply the inequality (9) we define

$$a = \sum_{k=1}^{N}\left(\frac{\sin^2\theta_k}{d_k^2\cos^2\phi_k} + \frac{\sin^2\phi_k\cos^2\theta_k}{d_k^2}\right) \tag{11a}$$

$$b = \sum_{k=1}^{N}\left(\frac{\cos^2\theta_k}{d_k^2\cos^2\phi_k} + \frac{\sin^2\phi_k\sin^2\theta_k}{d_k^2}\right) \tag{11b}$$

where a and b are both positive. Using

$$\frac{1}{a} + \frac{1}{b} \geqslant \frac{2}{\sqrt{a}\sqrt{b}} \tag{12a}$$

$$\frac{1}{2\sqrt{a}\sqrt{b}} \geqslant \frac{1}{a+b} \tag{12b}$$

we get

$$\frac{1}{a} + \frac{1}{b} \geqslant \frac{4}{a+b}. \tag{13}$$

$$\boldsymbol{\Phi} = \frac{1}{\sigma^2}\begin{bmatrix} \sum_{k=1}^{N}\left(\frac{\sin^2\theta_k}{d_k^2\cos^2\phi_k} + \frac{\sin^2\phi_k\cos^2\theta_k}{d_k^2}\right) & \sum_{k=1}^{N}\left(\frac{-\sin\theta_k\cos\theta_k}{d_k^2\cos^2\phi_k} + \frac{\sin^2\phi_k\sin\theta_k\cos\theta_k}{d_k^2}\right) & \sum_{k=1}^{N}\frac{-\sin\phi_k\cos\theta_k\cos\phi_k}{d_k^2} \\ \sum_{k=1}^{N}\left(\frac{-\sin\theta_k\cos\theta_k}{d_k^2\cos^2\phi_k} + \frac{\sin^2\phi_k\sin\theta_k\cos\theta_k}{d_k^2}\right) & \sum_{k=1}^{N}\left(\frac{\cos^2\theta_k}{d_k^2\cos^2\phi_k} + \frac{\sin^2\phi_k\sin^2\theta_k}{d_k^2}\right) & \sum_{k=1}^{N}\frac{-\sin\phi_k\sin\theta_k\cos\phi_k}{d_k^2} \\ \sum_{k=1}^{N}\frac{-\sin\phi_k\cos\theta_k\cos\phi_k}{d_k^2} & \sum_{k=1}^{N}\frac{-\sin\phi_k\sin\theta_k\cos\phi_k}{d_k^2} & \sum_{k=1}^{N}\frac{\cos^2\phi_k}{d_k^2} \end{bmatrix} \tag{7}$$

Substituting (13) into (9) gives

$$\sigma^2\left(\frac{1}{\sum\limits_{k=1}^{N}\left(\frac{\sin^2\theta_k}{d_k^2\cos^2\phi_k}+\frac{\sin^2\phi_k\cos^2\theta_k}{d_k^2}\right)}+\right.$$
$$\left.\frac{1}{\sum\limits_{k=1}^{N}\left(\frac{\cos^2\theta_k}{d_k^2\cos^2\phi_k}+\frac{\sin^2\phi_k\sin^2\theta_k}{d_k^2}\right)}+\frac{1}{\sum\limits_{k=1}^{N}\frac{\cos^2\phi_k}{d_k^2}}\right)\geqslant \tag{14}$$
$$\sigma^2\left(\frac{4}{\sum\limits_{k=1}^{N}\left(\frac{1}{d_k^2\cos^2\phi_k}+\frac{\sin^2\phi_k}{d_k^2}\right)}+\frac{1}{\sum\limits_{k=1}^{N}\frac{\cos^2\phi_k}{d_k^2}}\right)$$

where the equality holds when $a = b$. A solution for $a = b$ is that $2\theta_k$ have equal angular distribution, which also satisfies (10) if $N \geq 3$. In this paper we assume all sensors have the same absolute elevation angle from the target, $|\phi_1| = |\phi_2| = \cdots = |\phi_N|$.

Now the optimization problem becomes how to minimize the right side of the inequality (14). Let $c_k = \cos^2\phi_k$. Based on (9) and (14) we get

$$\text{tr}(CRLB) \geqslant \sigma^2\left(\frac{4}{\sum\limits_{k=1}^{N}\left(\frac{1}{d_k^2 c_k}+\frac{1-c_k}{d_k^2}\right)}+\frac{1}{\sum\limits_{k=1}^{N}\frac{c_k}{d_k^2}}\right). \tag{15}$$

Under the constraints that $d_1 = d_2 = \cdots = d_N$, $|\phi_1| = |\phi_2| = \cdots = |\phi_N|$ and the $2\theta_k$ have equal angular distribution, the inequality (15) becomes

$$\text{tr}(CRLB) = \sigma^2\frac{d_k^2}{N}\frac{3c_k^2+c_k+1}{-c_k^3+c_k^2+c_k}. \tag{16}$$

Also we know $c_k \in (0, 1]$. In order to get the smallest $\text{tr}(CRLB)$, we first calculate the derivative of the right side in (16) with respect to c_k and set it equal to zero:

$$\sigma^2\frac{d_k^2}{N}\frac{3c_k^4+2c_k^3+5c_k^2-2c_k-1}{(-c_k^3+c_k^2+c_k)^2} = 0 \tag{17}$$

from which the only real arithmetical solution is obtained as $c_k = 0.547282350699011$. Thus $\text{tr}(CRLB)$ will reach the minimum bound with the optimal sensors elevation angle $\phi_k = \pm 42.2868668755864^o$. Therefore the optimal sensor deployment is given by

$$\phi_k = \pm 42.2869^o$$
$$\theta_k = \begin{cases} \frac{360^o}{N}(k-1)+\theta_0, & \text{if } \phi_k = 42.2869^o \\ \frac{360^o}{N}(k-1)-180^o+\theta_0, & \text{otherwise} \end{cases} \tag{18}$$

where θ_0 can be any constant angle, $k = 1, 2, 3, ..., N$ and $N \geq 3$. Note that for $N = 2$ it is not possible to find θ_1 and θ_2 that will satisfy (10).

Furthermore, from (16) it is easy to see that if we increase the number of sensors N and deploy them closer to the target, the $\text{tr}(CRLB)$ will be smaller leading to a better estimation performance.

4. SIMULATION STUDIES

4.1. Target location estimator

In order to verify the effectiveness of the proposed optimality criterion, we design a simple AOA localization system that can be used to evaluate the estimation performance. As the 3D AOA target localization has a nonlinear measurement equation, an extended Kalman filter (EKF) is used. Here the target state vector is defined as

$$\boldsymbol{X} = [x_e, \dot{x_e}, y_e, \dot{y_e}, z_e, \dot{z_e}]^T \tag{19}$$

where $\dot{x_e}, \dot{y_e}, \dot{z_e}$ are the target velocity. In this paper we assume the target is stationary thus $\dot{x_e}, \dot{y_e}, \dot{z_e}$ are all zeros. The EKF algorithm based on the state-space equations is given by [4]:

$$\boldsymbol{X}_{k+1|k} = \boldsymbol{F}_k\boldsymbol{X}_{k|k} \tag{20a}$$
$$\boldsymbol{P}_{k+1|k} = \boldsymbol{F}_k\boldsymbol{P}_{k|k}\boldsymbol{F}_k^T \tag{20b}$$
$$\boldsymbol{z}_k = [\theta_k, \phi_k]^T + \boldsymbol{n}_k \tag{20c}$$
$$\boldsymbol{K}_k = \boldsymbol{P}_{k+1|k}\boldsymbol{H}_k^T(\boldsymbol{H}_k\boldsymbol{P}_{k+1|k}\boldsymbol{H}_k^T + \boldsymbol{R}_k)^{-1} \tag{20d}$$
$$\boldsymbol{P}_{k+1|k+1} = (\boldsymbol{I} - \boldsymbol{K}_k\boldsymbol{H}_k)\boldsymbol{P}_{k+1|k} \tag{20e}$$
$$\boldsymbol{X}_{k+1|k+1} = \boldsymbol{X}_{k+1|k} + \boldsymbol{K}_k(\boldsymbol{z}_k - \boldsymbol{h}_{k+1|k}) \tag{20f}$$
$$\boldsymbol{h}(\boldsymbol{X}_{k+1|k}) = \left[\arctan\left(\frac{\Delta y}{\Delta x}\right), \arctan\left(\frac{\Delta z}{d_{xyk}}\right)\right]^T \tag{20g}$$

where $\boldsymbol{F}_k$ is the state transform matrix

$$\boldsymbol{F}_k = \begin{bmatrix} 1 & T & 0 & 0 & 0 & 0 \\ 0 & 1 & 0 & 0 & 0 & 0 \\ 0 & 0 & 1 & T & 0 & 0 \\ 0 & 0 & 0 & 1 & 0 & 0 \\ 0 & 0 & 0 & 0 & 1 & T \\ 0 & 0 & 0 & 0 & 0 & 1 \end{bmatrix},$$

$\boldsymbol{h}(\cdot)$ is the nonlinear measurement function, $\boldsymbol{H}_{k+1|k}$ is the Jacobian of $\boldsymbol{h}(\boldsymbol{X}_{k+1|k})$, and $\boldsymbol{P}_{\boldsymbol{k|k}}$ is the Kalman covariance matrix which can be used to evaluate the estimation performance. We use T to denote the constant time interval between measurements. The matrix $\boldsymbol{R}_k$ is the angle measurement noise covariance which is impacted by the target range [17]:

$$\boldsymbol{R}_k = \text{diag}[\sigma_u^2 d_k^\gamma, \sigma_u^2 d_k^\gamma] \tag{21}$$

where σ_u means the unit distance squared error and γ is the power loss exponent. Here because we assume $\sigma_\theta = \sigma_\phi$, the unit squared errors are the same for θ_k and ϕ_k.

Assuming N sensors in the target localization system, the estimator will process sensor measurements one-by-one starting from the first sensor.

4.2. Numerical examples

We simulate a multi-sensor AOA target localization scenario with a stationary target located at $[1000, 1000, 1000]m$ using the target location estimator in the previous subsection. The initial parameters of the EKF are $\boldsymbol{X}_{0|0} = [1200, 0, 800, 0, 1400, 0]^T$ and $\boldsymbol{P}_{0|0} = \text{diag}[100^2, 0, 100^2, 0, 100^2, 0]$. Besides, $\gamma = 0.2$, $\sigma_u = 1$ degree and $T = 2$ seconds. To evaluate the estimation performance, the mean squared error (MSE) is calculated by using the trace of the covariance matrix $\boldsymbol{P}_{k+1|k+1}$ in (20).

Fig. 2(a) shows 100 sensors deployed with the same angular spacing and distance from the target but at different heights giving different ϕ_k. Actually, all the sensors are on the surface of a sphere forming different circles at different heights. Figs. 2(b) and (c) show the comparison of the MSE corresponding to different groups of sensors with diverse elevation angles. From Figs. 2(b) and (c) we can see that sensors with $\phi_k = 42.2869^o$ obtain the smallest MSE when all the sensor measurements have been processed. The sensors with $\phi_k = 42.2869^o$ satisfy the optimal deployment requirements in (18). Also the evolutions of MSE show a decreasing tendency as more measurements are used for estimation. The final MSE values in Table 1 also confirm the proposed optimal sensor deployment criterion.

Fig. 3 provides a comparison by using different sensor groups with different distances from the target and same θ_k distribution with all the elevation angles equal to 42.2869^o. A smaller MSE is achieved when the sensors are all located closer to the target as shown in Fig. 3(b). The final MSE values are $2.83, 7.34, 15.66$ and 27.90 for $260m, 440m, 620m$ and $800m$, respectively.

Finally we change the number of sensors with all the elevation angles equal to 42.2869^o. Figs. 4(a) and (b) show the sensor distribution and comparison of MSEs, respectively. We observe that a smaller MSE is achieved when more sensors are used. In Fig. 4(b) the final MSEs are $27.90, 47.65$ and 152.30 for $100, 60$ and 20 sensors, respectively.

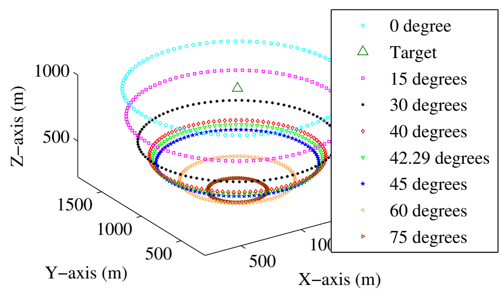

(a)

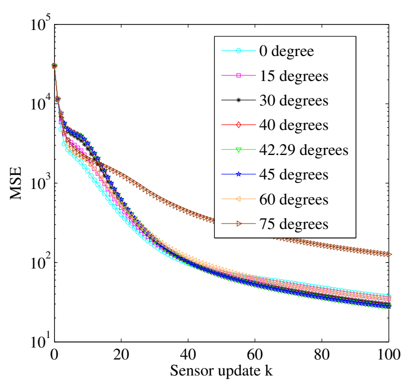

(b)

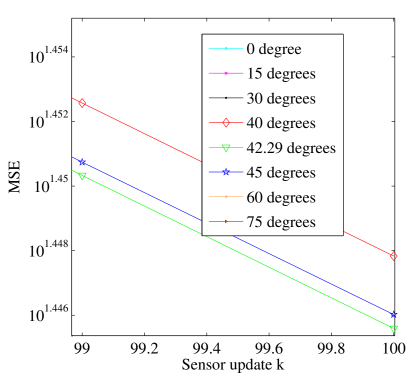

(c)

Fig. 2: (a) 100 sensors with different elevation angles but same distance. (b) Evolution of MSE. (c) Final MSE.

Table 1. Comparison of different elevation angles

Amount of sensors	Distance(m)	ϕ	Final MSE
100	800	0^o	36.94
100	800	15^o	34.97
100	800	30^o	30.05
100	800	40^o	28.04
100	800	42.29^o	27.90
100	800	45^o	27.93
100	800	60^o	35.27
100	800	75^o	126.70

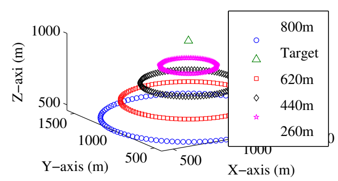

(a)

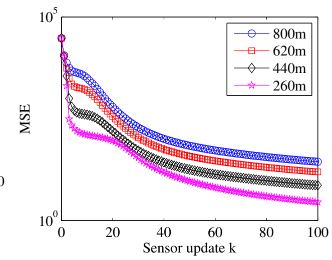

(b)

Fig. 3: (a) 100 sensors deployed with same elevation angle but different distances. (b) Evolution of MSE.

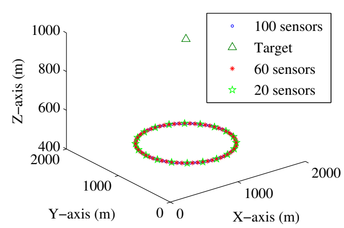

(a)

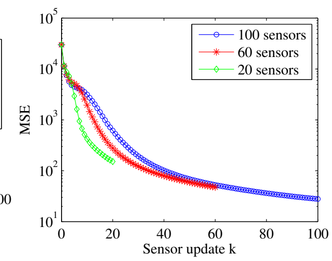

(b)

Fig. 4: (a) Different numbers of sensors deployed with same elevation angle and distance. (b) Evolution of MSE.

5. CONCLUSION

In this paper we have investigated optimal sensor placement strategies for 3D AOA target localization when all sensors have the same absolute elevation angle from the target. A novel and simple optimal sensor deployment criterion has been proposed based on minimizing the trace of CRLB (the A-optimality criterion). We showed that sensor elevation angles of $\pm 42.2869^o$ with twice of azimuth angles uniformly spaced gives an optimum geometry when the target is equidistant from the sensors and angle noise is i.i.d. The sign ambiguity allows for a multitude of optimal geometries. The effectiveness of the criterion has been verified by simulation examples utilizing an extended Kalman filter location estimator. The future work will consider 3D localization scenarios when sensor placed in different heights with different noise variances and nonuniform target range.

6. REFERENCES

[1] R.G. Stansfield, "Statistical theory of DF fixing," *Journal of the Institution of Electrical Engineers-Part IIIA: Radiocommunication*, vol. 94, no. 15, pp. 762–770, 1947.

[2] A.G. Lingren and K. F. Gong, "Position and velocity estimation via bearing observations," *Aerospace and Electronic Systems, IEEE Transactions on*, vol. AES-14, no. 4, pp. 564–577, 1978.

[3] K. Doğançay, "Bias compensation for the bearings-only pseudolinear target track estimator," *Signal Processing, IEEE Transactions on*, vol. 54, no. 1, pp. 59–68, 2006.

[4] K. Spingarn, "Passive position location estimation using the extended Kalman filter," *Aerospace and Electronic Systems, IEEE Transactions on*, vol. AES-23, no. 4, pp. 558–567, July 1987.

[5] N. Peach, "Bearings-only tracking using a set of range-parameterised extended Kalman filters," *IEE Proceedings-Control Theory and Applications*, vol. 142, no. 1, pp. 73–80, 1995.

[6] K. Doğançay and G. Ibal, "Instrumental variable estimator for 3D bearings-only emitter localization," in *Intelligent Sensors, Sensor Networks and Information Processing Conference, 2005. Proceedings of the 2005 International Conference on*, Dec 2005, pp. 63–68.

[7] A.N. Bishop, B. Fidan, B. Anderson, K. Doğançay, and P.N. Pathirana, "Optimality analysis of sensor-target localization geometries," *Automatica*, vol. 46, no. 3, pp. 479–492, 2010.

[8] J.A. Fawcett, "Effect of course maneuvers on bearings-only range estimation," *Acoustics, Speech and Signal Processing, IEEE Transactions on*, vol. 36, no. 8, pp. 1193–1199, 1988.

[9] Y. Oshman and P. Davidson, "Optimization of observer trajectories for bearings-only target localization," *Aerospace and Electronic Systems, IEEE Transactions on*, vol. 35, no. 3, pp. 892–902, 1999.

[10] D. Uciński, *Optimal measurement methods for distributed parameter system identification*, Springer Science & Business, 2004.

[11] K. Doğançay and H. Hmam, "Optimal angular sensor separation for AOA localization," *Signal Processing*, vol. 88, no. 5, pp. 1248–1260, 2008.

[12] S.Y. Zhao, B.M. Chen, and T.H. Lee, "Optimal sensor placement for target localization and tracking in 2D and 3D," *International Journal of Control*, vol. 86, no. 10, pp. 1687–1704, 2013.

[13] D. Moreno-Salinas, A. Pascoal, and J. Aranda, "Sensor networks for optimal target localization with bearings-only measurements in constrained three-dimensional scenarios," *Sensors*, vol. 13, no. 8, pp. 10386–10417, 2013.

[14] L. Rui and K.C. Ho, "Elliptic localization: Performance study and optimum receiver placement," *Signal Processing, IEEE Transactions on*, vol. 62, no. 18, pp. 4673–4688, Sept 2014.

[15] D.J. Torrieri, "Statistical theory of passive location systems," *Aerospace and Electronic Systems, IEEE Transactions on*, vol. AES-20, no. 2, pp. 183–198, March 1984.

[16] R. Bellman, *Introduction to matrix analysis*, vol. 2nd edn, McGraw-Hill, New York, 1970.

[17] K. Doğançay, "UAV path planning for passive emitter localization," *Aerospace and Electronic Systems, IEEE Transactions on*, vol. 48, no. 2, pp. 1150–1166, 2012.